Modeling and Link Quality Assessment of THz Network Within Data Center

Noureddine Boujnah, Saim Ghafoor and Alan Davy

Waterford Institute of Technology
TSSG, Waterford, Ireland
Email: bnoureddine@tssg.org, sghafoor@tssg.org, adavy@tssg.org

***Abstract*—Terahertz band has gained enormous interest recently due to its wide bandwidth availability, and the data rate is reaching 100 Gbps are nowadays achievable. The current advancement in Terahertz technology is aiming to achieve the data rate up to 1 Terabit per second. However, the unique band characteristics introduce some issues related to the propagation channel like high path and absorption loss which increases with distance. Such limitations at one hand can limit the coverage and throughput. But, on the other hand, suits indoor environment such as data center, a data center geometry is used in this paper to design and model a network of THz nodes placed on the top of the data center racks, to increase network connectivity, THz reflectors are positioned on ceiling and walls. Through simulations, we show that it is possible to reduce the average number of interferers in the system and minimize bit error probability by using specific waveforms and planar antenna array with active variable elements.**

I. Introduction

Terahertz band offers free large bandwidth windows between 0.1 and 10 THz [1] [2]; it can guarantee high data throughput transmission compared to lower frequency bands such as mm-wave and microwave bands. The limiting factors of THz communication are mainly severe amplitude decay because of the frequency and the molecular absorption phenomena [3].

Terahertz band finds its application in a plethora of fields [4] [5]. Recently it was demonstrated the feasibility of using the frequency band at $300GHz$ using optical UTC-PD devices reaching a data rate of $100Gbps$ for point to point link with an acceptable bit error rate [6] [7]. This paper focuses on designing wireless network architecture for data center, taking advantage from high available bandwidth and THz wave peculiarities, motivated by recent studies on the feasibility of deploying THz network within data center such as [8] [4].

Our contribution in this paper is to propose a THz wireless network architecture specific for data center, consisting of N^2 top of the rack nodes(TOR) and reflectors placed at room ceiling and walls to increase nodes reachability and path diversity. At the physical layer, we propose the use of orthogonal waveforms where two pulses describe each transmitted symbol; we derive an analytical form of bit error probability under coherent detection assumption and in the presence of interferences. We also prove that by tuning antenna, waveform parameters together with path diversity we can reduce the number of possible collisions and the bit error probability significantly. Simulations show that it is possible to reduce the average number of interferers considerably after some optimizations as well as minimizing the bit error probability.

The remaining of this paper is organized as follow: In section II, a network architecture for data center scenario is proposed. In section III, physical model for THz link is presented, including waveform, the antenna, and the channel model. The THz link is evaluated in term of the average number of interferers and the bit error probability in section IV, in section V simulation of the proposed topology is presented, and link quality is assessed. Finally, we conclude our paper by section VI.

II. Network model

A uniform racks arrangement characterizes data center network; one rack hosts networking elements such as servers and storage units linked to each other by optical fibers. Designing THz network in the data center seems promising, as THz wireless links are flexible and characterized by high bandwidth [11] [12].

In this paper we consider a regular arrangement of the top of the rack nodes, figure 1 shows an example of 4×4 network topology. Perfect planar reflectors for THz waves are placed on the ceiling at $Z = H$ and on walls, at the same level of THz nodes, to increase connectivity, and especially to establish direct connexion with non-neighbors. Each node can be linked to any node in the network using the line of sight or via reflected path as shown in figure 2. For instance, if the direct link is blocked or high interference is detected, the receiver recommends the transmitter to send its data via a secondary path. The propagating distance between two nodes takes the following form:

$$d = \sqrt{(i^2 + j^2)D^2 + 4kH^2} \tag{1}$$

Where, $i, j \in \{0, 1, 2 \dots N-1\}$ and $k \in \{0, 1\}$, direct link is possible when $i = 1$ and $k = 0$, H is the minimum distance separating reflectors plane to nodes. Placing reflectors at ceiling and walls increases node connectivity and offers several paths to reach destination, however, interference can occurs using this topology. We will optimize the network

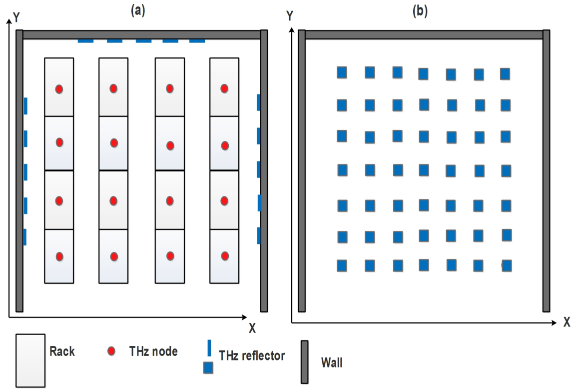

Fig. 1. (a) Top View of the data center network with reflectors placed on the ceiling (b) Arrangement of THz reflectors placed on the data center ceiling

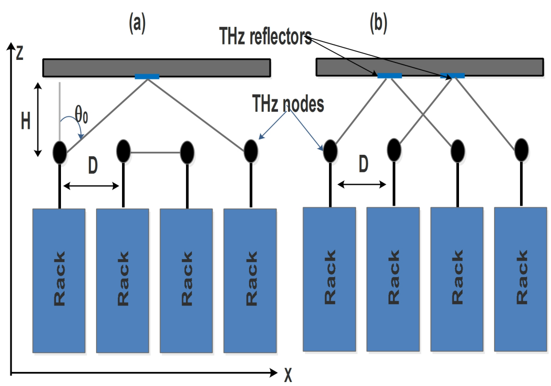

Fig. 2. (a) one direct P2P link and one reflected P2P link (b) Two reflected P2P links

parameters to reduce the average number of interferers and bit error probability.

III. Physical Layer Model

A. THz Waveform

Waveform for THz communication was proposed in [20], the transmitted signal consists of pulses placed in different positions within a symbol period. In this paper, we propose to design orthogonal waveforms to characterize each transmitter as well as to reduce interferences at receiver site, each node stores, in its memory, all the possible waveforms it can use to decode signals coming from other nodes. We design waveforms by placing two pulses in different positions within a symbol period to characterize the transmitted symbol, the symbol can take two states: $'0'$,as a silence, and $'1'$ presented by two consecutive pulses. The pulse duration is at least equal to $100fs$ [10], pulses positions within a symbol period and separations can be optimized to guarantee waveforms orthogonality and to reduce collisions at the receiving side. Similar method proposed in [13] but for non coherent reception and for nano-communication, where node position is not fixed. The transmitted signal from node i takes the form:

$$s_i(t) = \sqrt{P_{tx}} \sum_{l=0}^{\infty} a_l w_i(t - lT_s) \tag{2}$$

Where $a_l \in \{0, 1\}$ is the transmitted symbol, P_{tx} is the output power and $\{w_i(t)\}$ is a set of orthogonal waveforms that we propose in this paper:

$$w_i(t) = p(t - \delta_i T_p) + p(t - (\delta_i + \Delta_i)T_p) \tag{3}$$

Where, T_p is the pulse duration, p is the THz pulse, δ_i and Δ_i are two positive integers, T_s is the symbol duration given by $T_s = \kappa T_p$, where $\kappa \in \mathbb{N}$. Based on the orthogonality assumption between two different waveforms, we can write:

$$\begin{cases} \int_0^{T_s} w_i(t) w_j(t) dt = 0 \quad if & i \neq j \\ 1 & else \end{cases} \tag{4}$$

We assume that the transmitted pulse verifies:

$$\int_{-\frac{T_p}{2}}^{\frac{T_p}{2}} p(t)^2 dt = \frac{1}{2} \tag{5}$$

Then for $i \neq j$, the set of conditions that waveform parameters should meet are:

$$\begin{cases} \delta_i \neq \delta_j \\ \Delta_i + \delta_i \neq \delta_j \\ \delta_i + \Delta_i \neq \delta_i + \Delta_i \end{cases} \tag{6}$$

The motivation of this choice is to assign to each node a waveform that can be easily recognized at the receiving side using the value of Δ.

- By retrieving the pulse spacing Δ_i from the received signal, the receiver identifies and synchronizes with the transmitter. We assume that the receiver is endowed with such capability.
- Selection of a new waveform by the transmitter, if interference occurs or the bit error probability increase. Feedback messages from the receiver can contains a command to change the waveform.
- The same power when using a single pulse transmission is distributed between two pulses.
- The waveform can be adaptively reused by two nodes and if there is no plan of symmetry between them containing reflector or node.

The figure 3 describes two examples of overlapping and non-overlapping scheme of the proposed waveforms, with the non-overlapping scheme, we can build up to $\Upsilon = \lfloor \frac{\sqrt{9+8(\kappa+1)}-3}{2} \rfloor$ waveforms verifying Eq.6. For a network with N^2 nodes, we have : $\Upsilon > N^2$, then:

$$\kappa_{min} = \frac{(2N^2+3)^2 - 9}{8} \tag{7}$$

The average achieved data rate per node is then:

$$\frac{1}{N\kappa_{min}T_p} = \frac{2}{N^3(N^2+3)T_p} \tag{8}$$

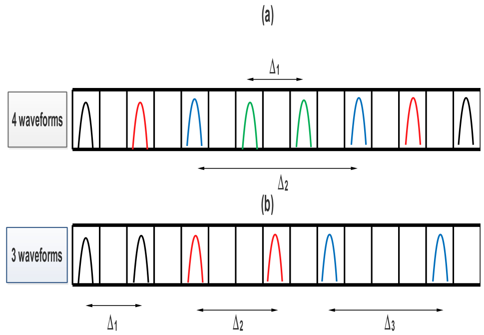

Fig. 3. (a) Overlapping scheme (b) Non-overlapping scheme

B. Antenna model

To overcome noise and propagation losses in THz domain and to mitigate limitations of THz devices in term of output power and receiver sensitivity, phased array antenna deemed to be the suitable solution to maximize the total link budget by increasing antenna gain [16] [17]. In this paper, we assume a 2D uniform array antenna with variable number of active elements. The array factor of an uniform planar array is given by [18]:

$$\psi_{ik}(\theta,\phi) = G\frac{\sin\left(M_a\frac{\pi f \xi}{c}[\sin(\theta)\cos(\phi)-\sin(\theta_{ik})\cos(\phi_{ik})]\right)}{\sin\left(\frac{\pi f \xi}{c}[\sin(\theta)\cos(\phi)-\sin(\theta_{ik})\cos(\phi_{ik})]\right)} \frac{\sin\left(N_a\frac{\pi f \xi}{c}[\sin(\theta)\sin(\phi)-\sin(\theta_{ik})\sin(\phi_{ik})]\right)}{\sin\left(\frac{\pi f \xi}{c}[\sin(\theta)\sin(\phi)-\sin(\theta_{ik})\sin(\phi_{ik})]\right)} \quad (9)$$

Where, G stands for the antenna element gain, $M_a \times N_a$ is the total number of active antenna elements, ξ is the spacing between two adjacent elements for each direction, its value is lower than the wavelength $\lambda = \frac{c}{f}$, θ_0 and ϕ_0 are the vertical and horizontal steering angles respectively.

Increasing the number of active antennae enhances link budget however it can increase interferences.

C. Channel model

Few channel models are available for THz band, the model depends on the propagation environment and its physical properties [19] [3]. The THz signal is subject to power attenuation, including spreading attenuation and molecular absorption, reflexions and additive noise. The received power from the main path between two nodes is:

$$P_r(f,d) = (GM_aN_aM_a^{'}N_a^{'})^2 P_t l(d,f) \quad (10)$$

Where, $M_a^{'} \times N_a^{'}$ is the number of antenna elements at the receiving side. $l(d,f)$ is the channel power attenuation, for THz frequency it is given by:

$$l(d,f) = \left(\frac{c}{4\pi f d}\right)^2 e^{-a(f)d} \quad (11)$$

$a(f)$ is an attenuation coefficient depending on frequency f and atmospheric parameters. Deeper study on channel modeling for THz band can be found in [15] [14]. $a(f)$ can be calculated using the HITRAN data base.

The received signal from node i at node k in presence of interferences is:

$$r_{i,k}(t) = g_{i,k}(d_{ik},f)s_i(t-\frac{d_{ik}}{c}) + I_{i,k}(t) + n_i(t) \quad (12)$$

Where $I_{i,k}(t)$ is the interferences during a symbol period:

$$I_{i,k}(t) = \sum_{j}^{N_I} g_{j,k}(d_{jk},f)s_j(t-\frac{d_{jk}}{c}) \quad (13)$$

where N_I is the total number of interferers during a symbol period, including reflected signal from the transmitter and signals coming from other nodes, $n_i(t)$ is assumed to be additive Gaussian noise, finally, the link gain g_{ik} is expressed as:

$$g_{i,k}(d,f) = \gamma(f)\sqrt{l(d,f)}\psi_t(\theta_{ik}^{(t)},\phi_{ik}^{(t)})\psi_r(\theta_{ik}^{(r)},\phi_{ik}^{(r)}) \quad (14)$$

Where t and r stand for transmitter and receiver. $\gamma(f)$ is the reflexion coefficient [9], $\gamma(f) = 1$ for line of sight path and for the reflected path, $\gamma(f)$ depends on the reflectors material and frequency, for perfect reflector $\gamma(f) = -1$.

IV. THz Link quality

In this paper, we will derivate the general form of the probability of errors and optimize its value for a given detection threshold. The interference model for wireless THz data center is different from the model proposed in [21] where stochastic geometry is used and nodes are distributed randomly.

A. Bit Error Probability

Under coherent reception assumption, waveform used by the transmitter can be recognized by the receiver after the link establishment phase, then the received signal during a symbol period $[T_l, T_{l+1}]$is calculated as:

$$r_{i,k} = \int_{T_l}^{T_{l+1}} r_{i,k}(t)w_i(t)dt \quad (15)$$

$r_{i,k}$ can be split into two terms:

$$r_{i,k} = r_{i,k}^{(1)} + r_{i,k}^{(2)} \quad (16)$$

Where:

$$\begin{cases} r_{i,k}^{(1)} = & \frac{1}{2}a_l g_{ik}\sqrt{P_t} + I_{i,k}^{(1)} + n_i^{(1)} \\ r_{i,k}^{(2)} = & \frac{1}{2}a_l g_{ik}\sqrt{P_t} + I_{i,k}^{(2)} + n_i^{(2)} \end{cases} \quad (17)$$

$I_{i,k}^{(1)}$ and $I_{i,k}^{(2)}$ can take positive as well as negative values and depend on the considered waveform. Assuming that interferences come from antenna side lobes, and only the strongest path will is considered. Decision at the receiver side is based on thresholding of $r_{i,k}^{(1)}$ and $r_{i,k}^{(2)}$.

The interference contribution ζ_{jk} of each node j is:

$$\zeta_{jk} = a_j\sqrt{P_{tx}}g_{jk}(d_{jk},f)\nu(\epsilon) \quad (18)$$

Where, a_j is the transmitted symbol by node j, and $\nu(\epsilon)$ the temporal correlation function between two pulses defined as:

$$\nu(\epsilon) = \int_{-\frac{T_p}{2}}^{\frac{T_p}{2}} p(t)p(t - \epsilon T_p)dt \qquad (19)$$

Where, $\epsilon \in [-1, 1]$ as described in Eq.27, ϵ depends on propagation delay difference between transmitter and interferers as well as on waveform parameters and pulse duration. From Eq.19 and Eq.5, it is possible to write: $\nu(\epsilon) \leq \frac{1}{2}$.

Let X be the receiver threshold to detect a pulse. The probability of correct detection at the receiver is given by:

$$\mathrm{P}_c(X) = 0.5Prob(r_{i,k}^{(1)} \geq X, r_{i,k}^{(2)} \geq X | a_l = 1) + 0.5Prob(r_{i,k}^{(1)} \geq X, r_{i,k}^{(2)} \geq X | a_l = 0) \qquad (20)$$

Using the fact that interferences depend on transmitted symbols, the mean value of the probability of receiving correct symbol $\bar{P}_c$ for a link (i, k), with respect to interferences, is:

$$\begin{aligned} \bar{P}_c(X) = 2^{-(N_I+1)} \textstyle\sum_{\zeta_1} \sum_{\zeta_2} \\ (Prob(r_{i,k}^{(1)}(\zeta_1) \geq X, r_{i,k}^{(2)}(\zeta_2) \geq X)|a_l = 1) \\ +Prob(r_{i,k}^{(1)}(\zeta_1) \leq X, r_{i,k}^{(2)}(\zeta_2) \leq X|a_l = 0)) \end{aligned} \qquad (21)$$

Where, $\hat{a}_k$ is the estimated value of the transmitted symbol after pulse detection. Let assume that the total number of interferers during a symbol duration is $N_I = N_I^{(1)} + N_I^{(2)}$, where $N_I^{(1)}$ and $N_I^{(2)}$ are the number of interferers affecting the first and the second pulse respectively, ζ_1 and ζ_2 are realization of interference affecting the first and the second pulse respectively, verifying:

$$\begin{cases} Prob(\zeta_1) & = 2^{-N_I^{(1)}} \\ Prob(\zeta_2) & = 2^{-N_I^{(2)}} \end{cases} \qquad (22)$$

For given ζ_1 and ζ_2,

$$\begin{aligned} Prob(r_{i,k}^{(1)}(\zeta_1) \geq X, r_{i,k}^{(2)}(\zeta_2) \geq X)|a_l = 1) = \\ \tfrac{1}{4}(1 - erf(\tfrac{X - \frac{1}{2}g_{ik}\sqrt{P_t} - \zeta_1}{\sqrt{2}\sigma_1})) \\ (1 - erf(\tfrac{X - \frac{1}{2}g_{ik}\sqrt{P_t} - \zeta_2}{\sqrt{2}\sigma_2})) \end{aligned} \qquad (23)$$

And,

$$\begin{aligned} {}_Prob(r_{i,k}^{(1)}(\zeta_1) \leq X, r_{i,k}^{(2)}(\zeta_2) \leq X)|a_l = 0) = \\ \tfrac{1}{4}(1 + erf(\tfrac{X - \zeta_1}{\sqrt{2}\sigma_3}))(1 + erf(\tfrac{X - \zeta_1}{\sqrt{2}\sigma_4})) \end{aligned} \qquad (24)$$

Where, $erf(x) = \frac{2}{\sqrt{\pi}} \int_0^x e^{-u^2} du$ the error function and, σ_1, σ_2, σ_3 and σ_4 are the standard deviations of the additive noise for each case. From Eq.21, notice that using physical parameters such as: receiver threshold X, number of active antenna elements and waveform shape it is possible to maximize P_c for a specific link. The main difference with the bit error rate formulated in [20] is that only noise is assumed to be Gaussian in our paper and interferences follow a uniform distribution among a finite set. The bit error probability is then given by:

$$P_e(X) = 1 - \bar{P}_c(X) \qquad (25)$$

When no interference occurs, the bit error probability becomes then:

$$\begin{aligned} P_e(X) = \\ 1 - \tfrac{1}{8}\left((1 + erf(\tfrac{\frac{1}{\sqrt{2}}g_{ik}\sqrt{P_t} - X}{\sqrt{2}\sigma_1}))^2 + (1 + erf(\tfrac{X}{\sqrt{2}\sigma_3}))^2\right) \end{aligned} \qquad (26)$$

B. Network optimization

An active node j can interfere with a communication link established between two nodes i and k, side lobes are the main source of interferences. Collisions occur if at least one of the four following time domain equations holds:

$$\begin{cases} \frac{d_{ik} - d_{jk}}{cT_p} & \equiv \quad \delta_i - \delta_j + \epsilon_1[\kappa] \\ \frac{d_{ik} - d_{jk}}{cT_p} & \equiv \quad \delta_i + \Delta_i - \delta_j + \epsilon_2[\kappa] \\ \frac{d_{ik} - d_{jk}}{cT_p} & \equiv \quad \delta_i - \delta_j - \Delta_j + \epsilon_3[\kappa] \\ \frac{d_{ik} - d_{jk}}{cT_p} & \equiv \quad \delta_i + \Delta_i - \delta_j - \Delta_j + \epsilon_4[\kappa] \end{cases} \qquad (27)$$

All direct and reflected paths between node i and k, and between j and k are considered, distance between nodes d_{ik} is described by Eq.1, $\epsilon_1, \epsilon_2, \epsilon_3, \epsilon_4 \in [-1, 1]$ when interference occurs. To reduce the number of equations verifying Eq.27, H describing positions of reflectors can be tuned, for example if H is shifted by small quantity h, the new reflected path length becomes:

$$d'_{jk} = \frac{4hH}{d_{jk}} + d_{jk} \qquad (28)$$

By tuning H and waveform parameters, it is possible to reduce the average number of interferers. Figure 4 describes the difference between traditional OOK modulation system using one pulse and our waveform design.

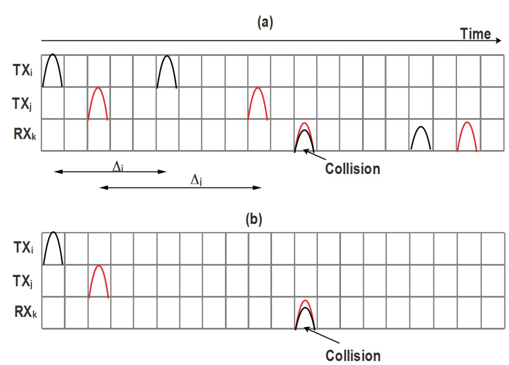

Fig. 4. (a) collision between two symbols(orthogonal waveforms) (b) Collision between two symbols in traditional OOK

Two levels of link quality assessment will be considered in this paper: average number of interferences evaluation and bit error probability computation.

V. Simulation results

We set up a network of $N \times N$ TOR nodes, reflectors are placed to increase connectivity, each node is assigned a unique waveform and equipped with a phased array antenna with variable active elements. Waveform selection, pulse and symbol duration, can also be tuned to reduce the number of interferers in the system. The simulation parameters are presented in table I.

TABLE I
SIMULATION PARAMETERS

Parameter	Value
Frequency	300 GHz
Interrack distance	$0.8m, 1.5m$
Network size	4×4,3×3 and 5×5
Pulse duration	$100fs$, $200fs$ $400fs$
P_t	$1mW$
H	$[0.8, 1.5]$
Temperature(Degree)	23
Humidity	15%
Antenna configuration	2×2,2×3, 3×3, 4×4

In figure 5 we plot the received power from transmitter and interferers. It is worth considering that interferences cn not be neglected for THz TOR network, and can contribute to signal quality degradation.

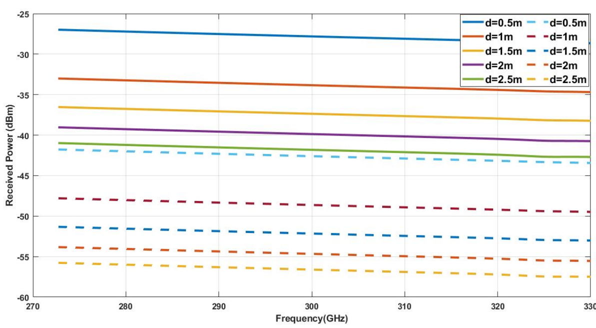

Fig. 5. Received power from 1 transmitter(continuous line) and 1 interferer(dashed line) for different distances, the antenna configuration used is 4×4

A. Average number of interferers

In figure 6 we study the impact of network size and symbol duration on the average number of interferers.

During the design phase, it is possible to select the appropriate waveform basis leading to a lower mean number of interferers, in figure 7, it is possible to select the best waveform allocation plan that reduce the average number of collisions. It is clear also that symbol duration affects the average number of interferers in the system. The average number of interferers depends mainly on the symbol and pulse duration and waveform selection, the bit error probability depends on antenna parameters, and distances.

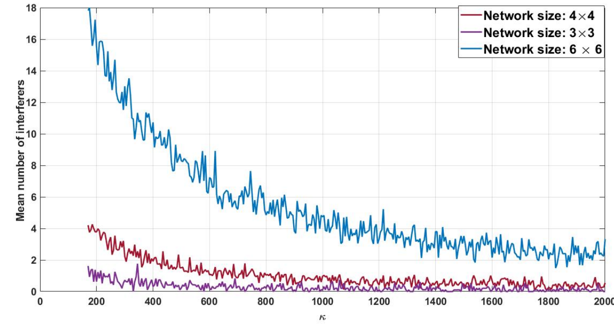

Fig. 6. Number of interferers as function of κ for 3 network topology

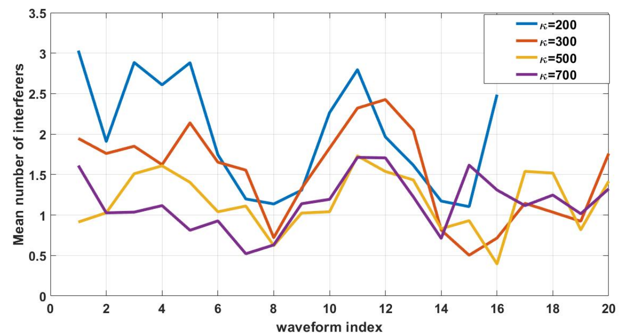

Fig. 7. Mean number of interferers as function of waveform selection

B. Bit error probability

The bit error probability is derived in subsection IV-A. We consider in our simulation one interferer per link. Figure 8 describes the bit error probability as a function of receiver threshold, by varying the number of active antenna elements of the interferer, it is possible to reach values of BER lower than 10^{-9}.

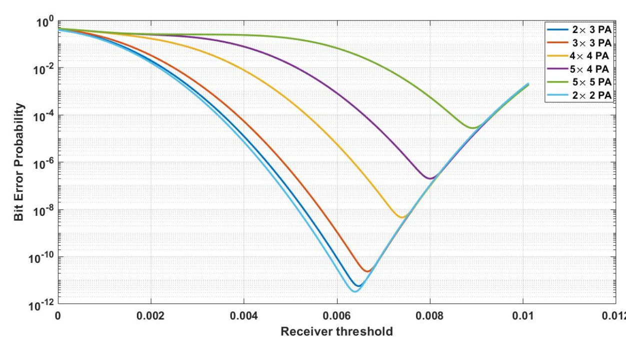

Fig. 8. Bit Error Probability for different antenna configuration of the interferer.

VI. Conclusion

In this paper, we proposed a network architecture for the THz data center consisting of uniform arrangement of nodes and reflectors to increase network visibility and path diversity, along with we proposed to use orthogonal waveforms to uniquely identify nodes at the receiving side and monitor interferences. To cope with channel impairments, uniform phased array with an adaptive number of elements is used, interference in the system is studied, and the bit error probability is derived and assessed. Link quality can be optimized by tuning some physical parameters. Simulation results show that we can build a THz network within a data center with a low average number of interferers and high connectivity, it is possible also to reach low bit error probability for the proposed waveform and for different antenna configurations. As perspectives, we will focus on pulse hopping for a larger data center network to reduce interferences and increase overall system capacity.

Acknowledgment

This work has received funding from the European Union's Horizon 2020 research and innovation programme under grant agreement No 761579 (TERAPOD)

References

[1] Tadao Nagatsuma *Terahertz Communications: Past, Present and Future* 40th International Conference on Infrared, Millimeter, and Terahertz waves (IRMMW-THz), 2015, Hong Kong, China.

[2] Ian F. Akyildiz, J.M. Jornet, C. Han *Terahertz band: Next frontier for wireless communications*, Journal of physical communication, , Vol. 12, 2014, p. 16-32.

[3] J. Jornet and I. Akyildiz, *Channel Modeling and Capacity Analysis for Electromagnetic Wireless Nanonetworks in the Terahertz Band* , IEEE Transactions on Wireless Communications,, vol. 10, no. 10, pp. 3211 3221, 2011.

[4] A.Davy, L.Pessoa, C.Renaud, E.Wasige, M.Naftaly, T. Krner, G.George, O.Cojocari, N. O' Mahony, M. A. G. Porcel, *Building an end user focused THz based ultra-high bandwidth wireless access network: The TERAPOD approach*, Ultra Modern Telecommunications and Control Systems and Workshops (ICUMT) 2017 9th International Congress on, pp. 454-459, 2017, ISSN 2157-023X

[5] S. S. Dhillon et al. *The 2017 terahertz science and technology roadmap* Journal of Physics D: Applied Physics, vol. 50, Number 4. 2017.

[6] Chinni, V. K., Zezaoui, M., Coinon, C., Wallart, X., Pevtavit, E., Larnpin, J. F., Ducournau, G. (2018). *Indoor* 100 *Gbit/s THz data link in the 300 GHz band using fast photodiodes*. 2018 25th International Conference on Telecommunications (ICT). doi:10.1109/ict.2018.8464945

[7] IEEE Std 802.15.3d *IEEE Standard for High Data Rate Wireless Multi-Media Networks, Amendment 2:* 100 *Gb/s Wireless Switched Point-to-Point Physical Layer*,2017

[8] Mollahasani, S., Onur, E. *Evaluation of terahertz channel in data centers*. NOMS 2016 - 2016 IEEE/IFIP Network Operations and Management Symposium.

[9] R. Piesiewicz, C. Jansen, D. Mittleman, T. Kleine-Ostmann, M. Koch, and T. Kurner, *Scattering analysis for the modeling of THz communication systems,* IEEE Trans. Antennas Propag., vol. 55, no. 11, pp. 3002-3009, Nov. 2007.

[10] J. M. Jornet and I. F. Akyildiz, *Femtosecond-long pulse-based modulation for terahertz band communication in nanonetworks,* IEEE Transactions on Communications, vol. 62, no. 5, pp. 17421754, 2014.

[11] T. Nagatsuma, S. Horiguchi, Y. Minamikata et al., *Terahertz wireless communications based on photonics technologies* Optics Express, vol. 21, no. 20, pp. 2373623747, 2013.

[12] J.Ma, R. Shrestha, L. Moeller, D.M. Mittelman *Channel performance for indoor and outdoor terahertz wireless links*APL Photonic3, 051601(2018).

[13] Singh, P., Kim, B.-W., Jung, S.-Y. *TH-PPM with non-coherent detection for multiple access in electromagnetic wireless nanocommunications* Nano Communication Networks(2018), 17, 113. doi:10.1016/j.nancom.2018.05.001.

[14] *Attenuation by atmospheric gases* Radiocommunication Sector of International Telecommunication Union. Recommendation ITU-R P.676-10, 2013.

[15] J.M. Jornet, I. F. Akyildiz, *Channel modeling and capacity analysis for electromagnetic wireless nanonetworks in the terahertz band*, IEEE Transactions on Wireless Communications, vol. 10, no. 10, pp. 3311-3221, 2011.

[16] Merkle, T., Tessmann, A., Kuri, M., Wagner, S., Leuther, A., Rey, S., Kurner, T. (2017). *Testbed for phased array communications from 275 to 325 GHz*. 2017 IEEE Compound Semiconductor Integrated Circuit Symposium (CSICS). doi:10.1109/csics.2017.8240474

[17] C. Lin, G. Y. Li, (2015). *Indoor Terahertz Communications: How Many Antenna Arrays Are Needed?* IEEE Transactions on Wireless Communications, 14(6), 30973107. doi:10.1109/twc.2015.2401560

[18] O. E. Ayach, S. Rajagopal, S. Abu-Surra, Z. Pi, and R. W. Heath Jr.,*Spatially sparse precoding in millimeter wave MIMO systems,* IEEE Trans. Wireless Commun., vol. 13, no. 3, pp. 1499-1513, Mar. 2014.

[19] Danping He, Ke Guan, Alexander Fricke, Bo Ai, Ruisi He, Zhangdui Zhong, Akifumi Kasamatsu, Iwao Hosako, Thomas Krner, *Stochastic Channel Modeling for Kiosk Applications in the Terahertz Band*, Terahertz Science and Technology IEEE Transactions on, vol. 7, pp. 502-513, 2017, ISSN 2156-342X

[20] C. Han, A.O. Bicen, I.F.Akyildiz *Multi-Wideband Waveform Design for Distance-Adaptive Wireless Communications in the Terahertz Band* IEEE TRANSACTIONS ON SIGNAL PROCESSING, VOL. 64, NO. 4, FEBRUARY 15, 2016

[21] Kokkoniemi J, Lehtomki J , Juntti M *Stochastic Geometry Analysis for Mean Interference Power and Outage Probability in THz Networks* IEEE Trans. Wireless Commun. pp. 3017 - 3028, 2017.